

Nuclear magnetic resonance of oriented ^{54}Mn nuclei in antiferromagnetic $\text{MnCl}_2 \cdot 4\text{H}_2\text{O}$

A. Kotlicki,* B. A. McLeod, M. Shott,[†] and B. G. Turrell

Department of Physics, University of British Columbia, Vancouver, British Columbia V6T2A6, Canada

(Received 29 August 1983)

NMR of oriented ^{54}Mn in antiferromagnetic $\text{MnCl}_2 \cdot 4\text{H}_2\text{O}$ has been studied by monitoring the change in γ -ray intensity. The strongest line has frequency 500.4 ± 0.1 MHz and weaker lines are observed at 503.5 ± 0.1 and 507.0 ± 0.5 MHz. The linewidth is 35 ± 5 kHz. A value for the hyperfine interaction strength $A = -203.8 \pm 0.1$ MHz is deduced. The 3.1-MHz splitting of the lines is due to second-order magnetic "pseudoquadrupole" interaction (2.7 MHz) and pure quadrupole interaction (0.4 MHz). Point-charge calculations agree fairly well with the latter value.

I. INTRODUCTION

The first observation of nuclear magnetic resonance of oriented nuclei in an antiferromagnet has been reported by Kotlicki and Turrell¹ who studied $^{54}\text{Mn}-\text{MnCl}_2 \cdot 4\text{H}_2\text{O}$. In this preliminary work a strong and sharp resonance was observed at 500.4 MHz. In this paper we report further measurements and present the experimental details and a full discussion of the results. In particular, using a Ge-Li detector we have observed higher frequency lines at 503.5 and 507 MHz. The shape of the line at 503.5 MHz is quite distinctive and very interesting, being due to the competing effects of the second and fourth rank tensor contributions to the γ -ray anisotropy and to effects of the ensuing spin-lattice relaxation. A preliminary account of this work has also been reported.²

The isotope ^{54}Mn is an excellent nucleus for nuclear orientation: it has spin $I=3$ and the measured values of the magnetic dipole and electric quadrupole moments are $\mu = +3.282\mu_N$ and $Q = +0.4$ b, respectively.³ It also has a simple decay first by electron capture to the 835-keV level of its daughter ^{54}Cr and then by $E2$ γ decay to the ground state.

The salt $\text{MnCl}_2 \cdot 4\text{H}_2\text{O}$ is a collinear antiferromagnet with a Néel temperature $T_N \simeq 1.6$ K and several studies have been made of its magnetic properties. The crystal structure is monoclinic ($\beta = 99.7^\circ$) with four magnetic ions per unit cell. The ionic positions and configurations have been determined by x-ray analysis⁴ and by neutron diffraction.⁵ The magnetic structure of the antiferromagnetic phase has been studied by NMR,⁶ neutron diffraction,⁷ and nuclear orientation.⁸ The easy axis of magnetization is known to be defined by polar angles $\theta = 8^\circ$ and $\phi = 3^\circ$ in the a^*bc coordinate frame.^{7,8} The molecular fields have been determined by susceptibility measurements,^{9,10} nuclear orientation,⁸ and specific-heat measurements.¹¹ The nuclear contribution in the specific-heat measurement indicated a hyperfine field of 64.5 T.

II. THEORY

A. Spin Hamiltonian and hyperfine interaction

Consider a system of ions with electronic spin S ordered collinearly by an exchange field B_E and under the influ-

ence of a crystalline field anisotropy interaction of strength D . Assume that the nuclear spins are oriented by an isotropic magnetic hyperfine interaction of strength A and that there is a much weaker electric quadrupole interaction. Regarding the latter interaction let the crystal axes X, Y, Z be the principal axes of the electric-field-gradient tensor V_{ij} where we choose

$$|V_{ZZ}| \geq |V_{YY}| \geq V_{XX}$$

and set $V_{ZZ} = eq$ and

$$\eta = (V_{XX} - V_{YY})/V_{ZZ}.$$

The nuclear-spin quantization axis z determined by the magnetic hyperfine interaction is defined by polar angles (θ, ϕ) in the crystal frame XYZ .

For the above system, the spin Hamiltonian is

$$H = g\mu_B B_E S_z + D[S_z^2 - \frac{1}{3}S(S+1)] + A \vec{I} \cdot \vec{S} + P[I_z^2 - \frac{1}{3}I(I+1)], \quad (1)$$

where the parameter

$$P = 3e^2qQ(3\cos^2\theta - 1 + 2\eta\sin^2\theta\cos 2\phi)/8I(2I-1).$$

Calculating to second order the separation of adjacent energy levels in the lowest hyperfine structure multiplet ($S_z = -\frac{5}{2}, I_z = m$) yields³

$$\begin{aligned} \Delta E_{m,m+1} &= E_{-5/2,m+1} - E_{-5/2,m} \\ &= -\frac{5}{2}A + \frac{\frac{5}{2}A^2m}{g\mu_B B_E - 4D} + P(2m+1). \end{aligned} \quad (2)$$

Note that the second and third terms in Eq. (2) have the same dependence on m : the third term is pure quadrupole and the second term is "pseudoquadrupole." It is important in $\text{MnCl}_2 \cdot 4\text{H}_2\text{O}$ because of the relatively high value of A and relatively low value of B_E .¹²

B. Nuclear orientation

In order to discuss the anisotropy of γ radiation emitted by oriented radioactive nuclei we assume that the magnetic part of the hyperfine interaction in Eq. (1) is so much greater than the quadrupole part that the effect of the latter may be neglected. Note, though, that the general

case has been discussed.¹³ For a collinear antiferromagnet in the absence of an applied field, the sublattice magnetization vectors lie parallel and antiparallel to the easy axis, and, at temperature T , the γ -ray intensity normalized to the warm count in a direction at angle α to the quantization axis (easy axis) is

$$W(\alpha) = \frac{1}{2} W(\alpha) + \frac{1}{2} W(\alpha + \pi) = \sum_{k \text{ even}} B_k U_k F_k P_k \cos(\alpha). \quad (3)$$

Here $U_k F_k$ are parameters related to the radioactive decay and P_k are the Legendre polynomials.¹⁴ The "orientation parameters" are given by¹⁴

$$B_k = \sum_M (2k+1)^{1/2} C(I, k, I; M, 0) p_M, \quad (4)$$

where $C(I, k, I; m, 0)$ are Clebsch-Gordan coefficients and p_m is the fractional population of the m th energy level which in thermal equilibrium is given by

$$p_m = \frac{\exp\left[\frac{5Am}{2k_B T}\right]}{\sum_m \exp\left[\frac{5Am}{2k_B T}\right]}. \quad (5)$$

For the 835-keV transition in the decay of ^{54}Mn the nuclear decay parameters are $U_2 F_2 = -0.495$ and $U_4 F_4 = -0.447$ and the normalized γ -ray intensity in the direction $\alpha = 0$ is

$$W(0) = 1 - (p_3 + p_{-3}) + 0.667(p_2 + p_{-2}) + 0.333(p_1 + p_{-1}). \quad (6)$$

Thus, as the nuclei are cooled the normalized intensity is reduced below the value unity. The quantity $\epsilon = 1 - W(0)$ is often called the " γ -ray anisotropy," although in many early nuclear orientations papers this name was given to the quantity $[1 - W(\pi/2)/W(0)]$.

C. Nuclear magnetic resonance of oriented nuclei (NMRON)

The population distribution among the $2I + 1$ levels can be changed by applying an electromagnetic field of frequency

$$\nu_{m, m+1} = \frac{1}{h} \Delta E_{m, m+1}. \quad (7)$$

The resonant absorption of energy from this radiofrequency (rf) field can be detected by monitoring the change in γ -ray intensity $W(\alpha)$. If the applied rf field b_1 is intense enough that the populations of the m and $m + 1$ levels are equalized (saturation) then the change in γ -ray intensity can be calculated. For $\alpha = 0$, Eq. (6) can be used to calculate the "signal" $\Delta W(0)_{m, m+1}$. For the case of ^{54}Mn the six resonance lines have frequency $\nu_{m+1, m}$ and strength

$\Delta W_{m, m+1} = -\Delta \epsilon_{m, m+1}$. Writing

$$\begin{aligned} \frac{5}{2} A^2 (g\mu_B B_E - 4D)^{-1} &= P', \\ h\nu_{-3-2} &= -\frac{5}{2} A - 3P' - 5P, \end{aligned} \quad (8a)$$

$$\begin{aligned} [\Delta W(0)]_{-3-2} &= 0.833(p_{-3} - p_{-2}), \\ h\nu_{-2-1} &= -\frac{5}{2} A - 2P' - 3P, \end{aligned} \quad (8b)$$

$$\begin{aligned} [\Delta W(0)]_{-2-1} &= -0.167(p_{-2} - p_{-1}), \\ h\nu_{-10} &= -\frac{5}{2} A - P' - P, \end{aligned} \quad (8c)$$

$$\begin{aligned} [\Delta W(0)]_{-10} &= -0.167(p_{-1} - p_0), \\ h\nu_{01} &= -\frac{5}{2} A + P, \\ [\Delta W(0)]_{01} &= 0.167(p_0 - p_1), \end{aligned} \quad (8d)$$

$$\begin{aligned} h\nu_{12} &= -\frac{5}{2} A + P' + 3P, \\ [\Delta W(0)]_{12} &= 0.167(p_1 - p_2), \end{aligned} \quad (8e)$$

$$\begin{aligned} h\nu_{23} &= -\frac{5}{2} A + 2P' + 5P, \\ [\Delta W(0)]_{23} &= 0.833(p_2 - p_3). \end{aligned} \quad (8f)$$

Note that in order to obtain significant signal strength it is necessary that the populations between adjacent levels be quite different, which means that $T \lesssim |A|/k_B$ [see Eq. (5)]. Since this also means that the lower the energy level the greater its population, the signal strengths $\Delta W(0)_{m, m+1}$ are quite different. Thus, for ^{54}Mn the strongest line at ν_{-3-2} is positive, i.e., there is an increase in $W(0)$ (decrease in ϵ), whereas the next two lines at ν_{-2-1} and ν_{-10} show a decrease in $W(0)$ or an enhancement of ϵ . However, we shall see that the response of the nuclear-spin system after resonance under the spin-lattice interaction produces some surprising effects. Note also that the above behavior is quite different from that observed in conventional NMR; there, it is usual that the high-temperature approximation $T \gg |A|/k_B$ applies and all the lines have the same sign and intensity. A very positive advantage of the NMRON experiment is that the sign of the effective quadrupole interaction can be determined: The pseudoquadrupolar part P' is positive and, if its magnitude is known, the sign and magnitude of P can be estimated.

The spin-lattice relaxation is treated by assuming a dynamic hyperfine interaction of the form

$$H(t) = A \vec{I} \cdot \delta \vec{S}(t). \quad (9)$$

Transitions then occur between adjacent energy levels and we assume that the changes in population are governed by a master equation

$$\begin{aligned} \frac{dp_m}{dt} &= p_{m+1} Q_{m+1, m} - p_m (Q_{m, m+1} + Q_{m, m-1}) \\ &\quad + p_{m-1} Q_{m-1, m}. \end{aligned} \quad (10)$$

The transition rates $Q_{m, n}$ from level m to level n can be defined in terms of a spin-lattice relaxation time T_1 and are

$$Q_{m,m+1} = \frac{1}{T_1} \frac{I(I+1) - m(m+1)}{1 + \exp(-5A/2k_B T_L)}, \quad (11a)$$

$$Q_{m+1,m} = \frac{1}{T_1} \frac{I(I+1) - m(m+1)}{1 + \exp(5A/2k_B T_L)}. \quad (11b)$$

Here T_L is the lattice temperature, and the recovery of the γ -ray anisotropy to the value appropriate to thermal equilibrium at that temperature can be calculated by solving Eq. (10) using Eqs. (11a) and (11b), and substituting into Eq. (6). This is best done numerically using a computer. Theoretical curves for the relaxation of $W(0)$ after the ν_{-3-2} and ν_{-2-1} transitions at $T_L = 80$ mK are shown in Fig. 1. Of particular interest is the shape of the relaxation curve after the ν_{-2-1} transition. The nuclear-spin system is initially in thermal equilibrium at lattice temperature T_L . At resonance there is a decrease in $W(0)$ (increase in ϵ) as given by Eq. (8b). Then as the rf field is swept off-resonance, the spin-lattice relaxation causes the $W(0)$ to increase to a maximum value *above* the thermal equilibrium value after which it decreases back to the thermal equilibrium value. This behavior was unexpected and serves as a signature to the resonance. Experimentally, the sharp decrease in $W(0)$ (increase in ϵ) will disappear if the modulation frequency is too great, in which case only a shallow hump of increased intensity is observed.

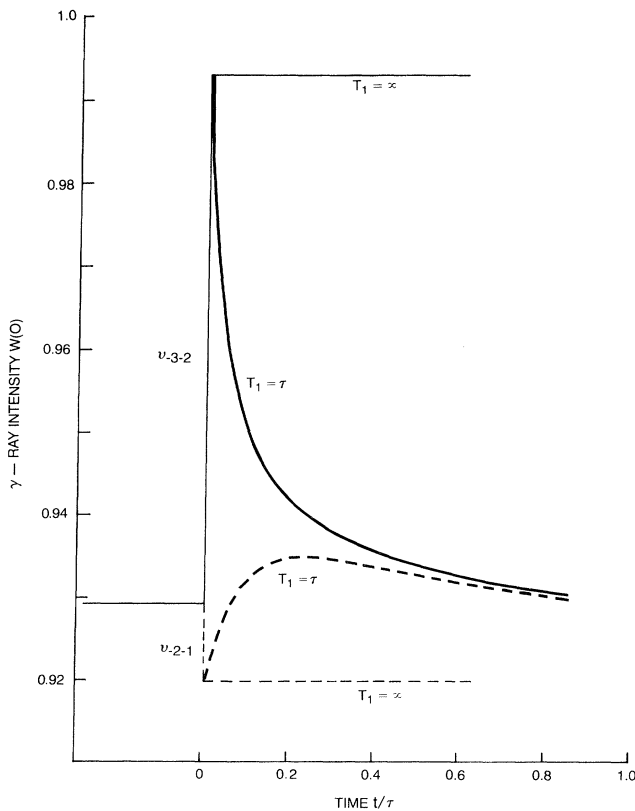


FIG. 1. Theoretical curves for the spin-lattice relaxation of the ^{54}Mn spins. At $t=0$ either the $M = -3 \rightarrow M = 2$ or the $M = -2 \rightarrow M = 1$ transition is excited by NMRON and then the system is allowed to relax to a lattice temperature $T_L = 80$ mK.

In the NMRON measurement of an antiferromagnet, just as in a conventional NMR experiment, there is enhancement of the applied rf field b_1 by a factor $(1 + \xi)$. Referring to Fig. 2, for b_1 applied perpendicular to the easy axis the sublattice magnetization vectors \vec{M}_1 and \vec{M}_2 are rotated through an angle β given by

$$\sin\beta = \frac{\chi_{\perp} b_1}{M_0} \simeq \frac{b_1}{B_E}, \quad (12)$$

where χ_{\perp} is the perpendicular susceptibility, $M_0 = |\vec{M}_1| = |\vec{M}_2|$, and we have assumed that the exchange field B_E is much greater than the crystalline anisotropy field. The rf field varying at frequency ν will cause the sublattice magnetization vectors to fluctuate at this frequency and the nuclei will feel an rf field, enhanced by hyperfine interaction, of value

$$b'_1 = b_1 + B_N \sin\beta = \left[1 + \frac{B_N}{B_E} \right] b_1. \quad (13)$$

Here $B_N = 5AI/2\mu$, and using $B_E = 12T$ and $B_N = 60T$ we calculate an enhancement factor

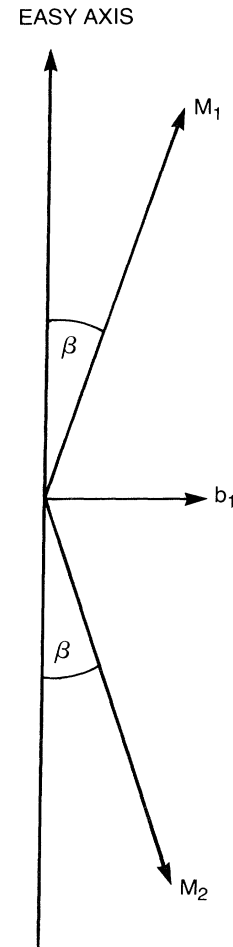


FIG. 2. Application of an rf field b_1 perpendicular to the easy axis tilts the sublattice magnetizations producing enhancement of b_1 at the nuclear site via hyperfine interaction.

$$\xi \approx \frac{B_N}{B_E} \approx 50$$

for $\text{MnCl}_2 \cdot 4\text{H}_2\text{O}$.

For a line of halfwidth $\Delta\nu$, the condition for saturation of the resonance is

$$(\mu/Ih)^2 b_1^2 (1 + \xi)^2 T_1 \geq 2 \Delta\nu. \quad (14)$$

For ^{54}Mn - $\text{MnCl}_2 \cdot 4\text{H}_2\text{O}$, $\mu/Ih \approx 8.33 \times 10^6$ rad/sec T, and so we require

$$b_1 \approx 5 \times 10^{-9} \left[\frac{\Delta\nu}{T_1} \right]^{1/2} T. \quad (15)$$

III. EXPERIMENT

Two crystals of $\text{MnCl}_2 \cdot 4\text{H}_2\text{O}$ were grown from a saturated solution containing radioactive ^{54}Mn . These crystals were platelike with the flat area containing the c and b crystalline directions. They had dimensions in the c , b , and a^* directions of approximately 15, 10, and 2 mm, respectively, and each had an activity of $\sim 5 \mu\text{Ci}$. The two crystals were tied with cotton thread to each side of a copper fin using Apiezon N grease for thermal contact. The fin was connected to the mixing chamber of a dilution refrigerator. The c axes were aligned vertically and a Ge-Li detector or a NaI detector was mounted to count γ -rays emitted in the downward vertical direction. (The Ge-Li counting system was used in long runs over wide frequency ranges because of its greater stability.) This meant that the measurements of γ -ray intensity were made at an angle $\alpha = 8^\circ$ [see Eq. (3)] to the quantization axis. However, the normalized intensity $W(\alpha)$ differs by only $\sim 3\%$ from $W(0)$. In these experiments no external steady magnetic fields were applied. The rf field was applied along the crystalline b axis by means of a coil placed on a plastic window in the 1-K copper shield of the dilution refrigerator. The power of the rf field needed to satu-

rate the resonance was such that some eddy current heating was produced in the fin which in turn warmed the crystals. Since the γ -ray anisotropy depends on temperature it was important to differentiate between changes in anisotropy due to the magnetic resonance and those due to eddy current heating. This problem was solved by maintaining the fin temperature closely constant by means of a carbon resistor attached to it close to the specimen and using this resistor as a feedback control to provide continuous adjustment of the rf level. We checked that during the frequency sweep through the range of interest the level of b_1 was sufficient to produce the maximum change in γ -ray anisotropy and that the anisotropy was changed very little in sweeps off-resonance.

The dilution refrigerator cooled the copper fin to about 15 mK and the specimen crystals reached a temperature ~ 50 mK. The specimen took many hours to cool due to the weak spin-lattice interaction and poor thermal contact at the fin crystal boundary. When the rf field was switched on the temperature rose to ~ 80 mK and the γ -ray anisotropy was $\epsilon \sim 0.07$. The frequency was swept upwards through the strongest resonance and we observed $\nu_{-3-2} = 500.4 \pm 0.3$ MHz in agreement with our earlier more accurate measurement¹ of $\nu_{-3-2} = 500.4 \pm 0.1$ MHz. A typical run is shown in Fig. 3. A run over the frequency range 497–509 MHz is shown in Fig. 4; note the sharp strong increase in γ -ray intensity at ν_{-3-2} and additional increases at frequencies of approximately 503.5 and 507 MHz. To study more closely the spectrum above ν_{-3-2} , runs were made either starting just above this frequency and sweeping upwards or starting well above and sweeping downwards. All these runs showed evidence of structure at 503.5 ± 0.1 MHz and at 507 ± 0.5 MHz. The line seen at 514.7 MHz in the earlier experiments¹ might possibly have been a higher frequency line, but more likely was a spurious effect resulting from an instability in the NaI counting system. A slower run with smaller modulation and better resolution displays the signature of the ν_{-2-1}

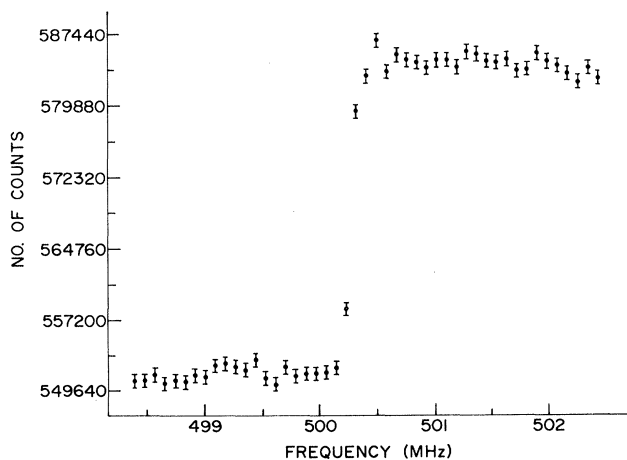


FIG. 3. The most intense NMRON line corresponding to the $M = -3 \rightarrow M = -2$ transition. These data were collected using a NaI detector system.

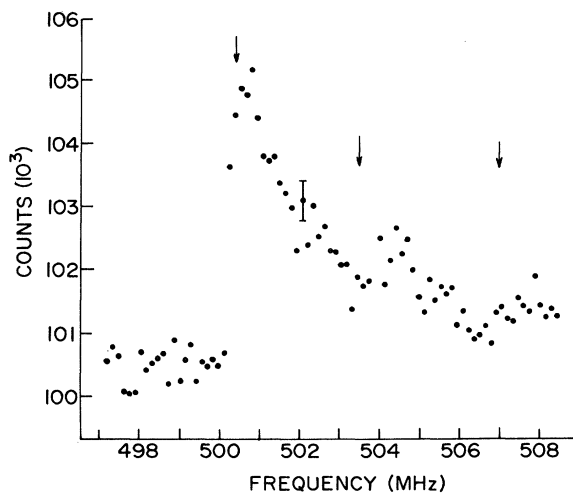


FIG. 4. A sweep over the range 497–509 MHz using a Ge-Li detector system. Arrows indicate the positions of the weaker $M = -2 \rightarrow M = -1$ and $M = -1 \rightarrow M = 0$ transitions at higher frequencies.

line, i.e., a sharp enhancement of the anisotropy followed by an overshoot of the equilibrium value. Actually, it is impossible to get a good theoretical fit to the raw data. However, if it is assumed that there is a slight warming effect through the run, as evidenced by the increase in counts before resonance, and a correction made for this, an excellent fit with the theoretical model is attained as shown in Fig. 5. We conclude then that $\nu_{-2,-1} = 503.5 \pm 0.1$ and $\nu_{-10} = 507.0 \pm 0.5$ MHz.

The linewidth of $\nu_{-3,-2}$ was obtained by monitoring the γ -ray intensity as the rf sweeper was advanced in 1.0 kHz steps with modulation frequency 1.5 kHz. This run is shown in Fig. 6 where each plotted point represents the average of eight consecutive raw datum points. Reanalyzing the data assuming a Gaussian distribution of resonance frequencies, we find that NMRON γ -intensity spectrum is best fitted with a halfwidth at half maximum $\delta\nu = 35 \pm 5$ kHz rather than the value of 60 kHz previously reported.¹

Our measurements of the spin-lattice relaxation do suggest that there may be size and/or impurity¹ effects. Thus, measurements on three crystals of increasing size yielded values for T_1 of $(2.0 \pm 0.3) \times 10^3$ sec, $(7 \pm 1) \times 10^3$ sec, and $(25 \pm 4) \times 10^3$ sec. However, we can draw no firm conclusions because T_1 certainly depends strongly on the lattice temperature which is difficult to estimate accurately.

We also investigated the strength of the NMRON signal as a function of rf field amplitude. An rf power meter was used to calibrate the rf level at the specimen site for the different output settings of the rf oscillator. For field amplitudes above 1.3×10^{-8} T a constant (maximum) NMRON signal $\Delta W(0)$ was obtained; below this field the signal fell off rapidly. In the experiments the oscillator was set to generate a field of $\sim 3 \times 10^{-8}$ T at the crystals. Using Eq. (15) we find that the saturation condition for

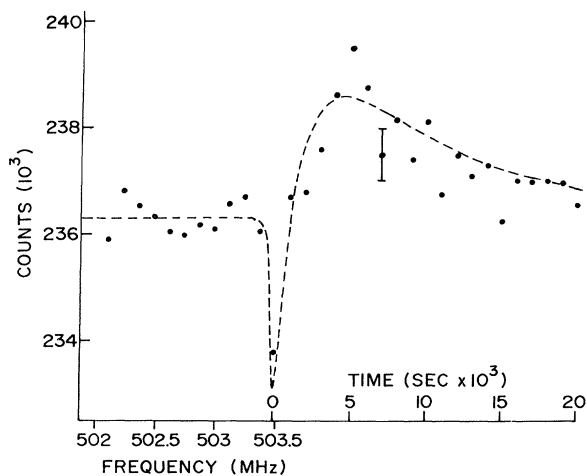


FIG. 5. $M = -2 \rightarrow M = -1$ transition. In this run the frequency was swept upward, with modulation 0.1 MHz, until the resonance occurred at $t=0$ and then swept off-resonance leaving the spin system to relax to the lattice temperature $T_L = 64$ mK. Dashed line is a theoretical curve (see Sec. IV B) using $T_1 = 2.4 \times 10^4$ sec.

$\Delta\nu = 35 \times 10^3$ Hz and $T_1 = 10^4$ sec requires $b_1 \geq 1 \times 10^{-8}$ T in good agreement with the above observations.

IV. DISCUSSION OF RESULTS

A. Quadrupole interaction

The separation of the resonant frequencies and the relative intensities of the lines allow us to deduce from Eqs. (8) that $(P' + 2P)/h = +3.1$ MHz. Using the value of $B_E - 4D/g\mu_B = 1.39 \pm 0.01$ T deduced from susceptibility measurements,⁹ we also calculate $A/h = -203.8 \pm 0.1$ MHz, $P'/h = 2.66 \pm 0.02$ MHz, and, hence, $P/h = 0.22 \pm 0.05$ MHz.

We have performed point-charge calculations of the electrostatic field gradient for two models. Model 1 is Baur's model¹⁵ for calculating the electrostatic energy per unit cell, which is consistent with neutron-diffraction studies:⁵ charges of $+2e$, $-e$, $-e$, and $+\frac{1}{2}e$ are allocated to the Mn, Cl, O, and H ions, respectively. In model 2, we assume the water molecules are completely neutral (no charge on either the O or H ions) and the Mn and Cl carry $+2e$ and $-e$, respectively.

For model 1 we find $q = -0.026 \times 10^{24}$ cm⁻³ and $\eta = 0.981$, with the X, Y, and Z axes coinciding with the (0.056, 0.681, -0.730), (-0.242, 0.718, 0.652), and (0.969, 0.140, 0.205) directions, respectively, in the a^*bc frame. From these results we calculate a value of $P/h = +0.072$ MHz, assuming that the antishielding factor $(1 - \gamma_\infty) = 9$ as given by Yasuoka *et al.*¹⁶

For model 2 we find $q = 0.128 \times 10^{24}$ cm⁻³ and $\eta = 0.746$ with the X, Y, and Z axes coinciding with the (-0.152, 0.882, 0.445), (-0.938, -0.271, 0.217), and

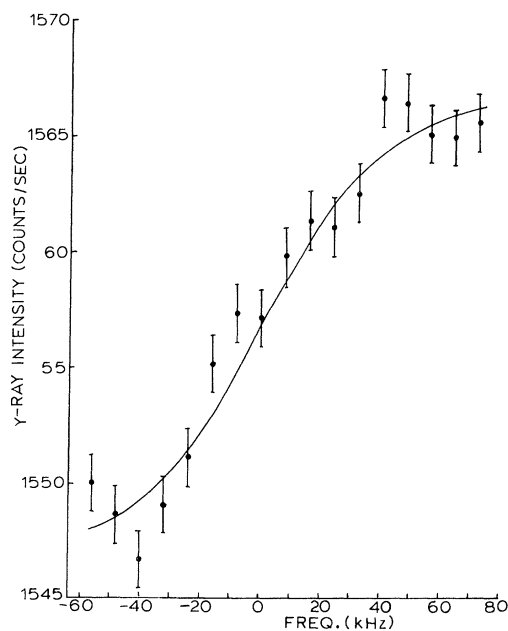


FIG. 6. Data obtained in a run in which the rf sweeper was advanced in 1 kHz steps with modulation 1.5 kHz. Each datum point is the average of eight consecutive steps. The line is the theoretical result assuming a Gaussian distribution of resonance frequencies with a HWHM of 35 kHz.

(0.312, -0.385 , 0.869) directions in the a^*bc frame. We calculate for this case $P/h = +0.63$ MHz assuming the same antishielding factor. Both calculated values of P are positive and the experimental value lies between them, which is satisfactory considering the simplicity of the models.

B. Hyperfine field and $\langle S_z \rangle$

The value of the magnetic hyperfine parameter deduced from our measurements is $A = -203.8$ MHz which corresponds to a hyperfine field of $B_N = -61.1$ T. Actually, there is a contribution from the dipolar field of all the other manganese ions which we estimate to be $+0.12$ T, a fairly small value due to the array of magnetic ions being close to cubic. Note that any contribution to a frequency shift from the Suhl-Nakamura interaction^{17,18} is negligible because the ^{54}Mn spins are very dilute ($\sim 3 \times 10^{13} \text{ cm}^{-3}$). Thus, the contribution to B_N from the $A\vec{S} \cdot \vec{I}$ interaction is -61.2 T, a value smaller than expected from results on other manganese ions. In MnF_2 and $\text{Mn}^{2+}\text{-ZnF}_2$ the values of B_N are 63.5 and 63.9 T, respectively.¹⁶ In fact, one would expect zero point deviation to cause the former value to be 2.4% less than the latter, but it is surmized that cation-cation interaction produces off-setting effects. The difference between the $\text{MnCl}_2 \cdot 4\text{H}_2\text{O}$ and $\text{Mn}^{2+}\text{-ZnF}_2$ is 4.2%. Zero point deviation (also 2.4%) would account for some of this difference. Crystal field effects from an ES_x^2 term in the spin Hamiltonian, Eq. (1), with $E = 1.2 \times 10^{-17} \text{ erg}^{10}$ would reduce $\langle S_z \rangle$ by a further 0.2%. The residual 1.6% remains a puzzle, although we

note that EPR measurements show a significant variation in the value of A for the Mn^{2+} ion in different hosts.¹⁹

C. Linewidth

The concentration of ^{54}Mn atoms in the sample is $\sim 2 \times 10^{13}$ atoms per cm^3 compared to $\sim 6 \times 10^{21}$ ^{55}Mn atoms per cm^3 . The Suhl-Nakamura interaction is an indirect coupling effective only between identical nuclear spins and its contribution to the ^{54}Mn linewidth is completely negligible. The measured linewidth of 35 kHz for the $-3 \rightarrow -2$ transition is relatively very narrow compared to the linewidth of ~ 500 kHz for ^{55}Mn in MnF_2 , for example.¹⁶ It is also interesting to note that in $^{55}\text{MnF}_2$ there is an extra broadening effect which is M dependent and is ~ 70 kHz for the outer $\frac{5}{2} \leftrightarrow \frac{3}{2}$ transitions. This effect is attributed at least partly to strain-induced quadrupolar broadening and it is tempting to suggest the same cause for the linewidth observed in our experiments.

ACKNOWLEDGMENTS

This work was supported by operating and equipment grants from the Natural Sciences and Engineering Research Council of Canada. Two of us (A.K. and M.S.) wish to thank Dr. D. L. Williams and members of the University of British Columbia Department of Physics for the hospitality extended to them during their visits. We acknowledge very useful discussions with Dr. N. J. Stone and Dr. R. G. Clark of the Clarendon Laboratory, Oxford. They pointed out to us the importance of the pseudoquadrupole interaction.

*Permanent address: Institute of Experimental Physics, Warsaw University, Hoza 69, PL-00-681 Warsaw, Poland.

†Permanent address: The Open University, Southern Region, Foxcombe Hall, Boars Hill, Oxford OX1 5HR, England.

¹A. Kotlicki and B. G. Turrell, *Hyperfine Interact.* **11**, 197 (1981).

²A. Kotlicki, B. A. McLeod, M. Shott, and B. G. Turrell, in *Proceedings of the VI International Conference on Hyperfine Interactions, Groningen, 1983* (in press).

³L. Niesen and W. J. Huiskamp, *Physica* **50**, 259 (1970).

⁴A. Zalkin, J. D. Forrester, and D. H. Templeton, *Inorg. Chem.* **3**, 529 (1964).

⁵Z. M. El Saffar and G. M. Brown, *Acta. Crystallogr. Sect. B* **27**, 66 (1971).

⁶R. D. Spence and V. Nagarajan, *Phys. Rev.* **149**, 191 (1966).

⁷R. F. Altman, S. Spooner, D. P. Landau, and J. E. Rives, *Phys. Rev. B* **11**, 458 (1975).

⁸R. L. A. Gorling, B. G. Turrell, and P. W. Martin, *Can. J. Phys.* **55**, 1526 (1977).

⁹J. E. Rives, *Phys. Rev.* **162**, 491 (1967).

¹⁰J. E. Rives and V. Benedict, *Phys. Rev. B* **12**, 1908 (1975).

¹¹A. R. Miedema, R. F. Wielinga, and W. J. Huiskamp, *Physica* **31**, 835 (1965).

¹²M. de Aránjo, G. J. Bowden, R. G. Clark, and N. J. Stone, in *Proceedings of the VI International Conference on Hyperfine Interactions, Groningen, 1983* (in press).

¹³G. J. Bowden, I. A. Campbell, N. Nambudripact, and N. J. Stone, *Phys. Rev. B* **20**, 352 (1979).

¹⁴R. J. Blin-Stoyle and M. A. Grace, *Handb. Phys.* **42**, 555 (1957).

¹⁵W. H. Baur, *Inorg. Chem.* **4**, 1840 (1965).

¹⁶H. Yasuoka, Tin Ngwe, and V. Jaccarino, *Phys. Rev.* **177**, 667 (1969).

¹⁷H. Suhl, *Phys. Rev.* **109**, 606 (1958).

¹⁸T. Nakamura, *Prog. Theor. Phys. (Kyoto)* **20**, 542 (1958).

¹⁹A. Abraham and B. Bleaney, *Electron Paramagnetic Resonance of Transition Ions* (Oxford University Press, London, 1970).